Design and analysis of a 3D-flux flux-switching permanent magnet machine with SMC cores and ferrite magnets

Chengcheng Liu, Youhua Wang, Gang Lei, Youguang Guo, and Jianguo Zhu

Citation: AIP Advances **7**, 056632 (2017); doi: 10.1063/1.4974524
View online: https://doi.org/10.1063/1.4974524
View Table of Contents: http://aip.scitation.org/toc/adv/7/5
Published by the American Institute of Physics

Design and analysis of a 3D-flux flux-switching permanent magnet machine with SMC cores and ferrite magnets

Chengcheng Liu,[1,a] Youhua Wang,[1,a] Gang Lei,[2] Youguang Guo,[2] and Jianguo Zhu[2]
[1]*Province-Ministry Joint Key Laboratory of EFEAR, Hebei University of Technology, Tianjin 300130, China*
[2]*School of Electrical, Mechanical and Mechatronic System, University of Technology Sydney, Sydney 2007, Australia*

(Presented 4 November 2016; received 6 September 2016; accepted 28 October 2016; published online 17 January 2017)

Since permanent magnets (PM) are stacked between the adjacent stator teeth and there are no windings or PMs on the rotor, flux-switching permanent magnet machine (FSPMM) owns the merits of good flux concentrating and robust rotor structure. Compared with the traditional PM machines, FSPMM can provide higher torque density and better thermal dissipation ability. Combined with the soft magnetic composite (SMC) material and ferrite magnets, this paper proposes a new 3D-flux FSPMM (3DFFSPMM). The topology and operation principle are introduced. It can be found that the designed new 3DFFSPMM has many merits over than the traditional FSPMM for it can utilize the advantages of SMC material. Moreover, the PM flux of this new motor can be regulated by using the mechanical method. 3D finite element method (FEM) is used to calculate the magnetic field and parameters of the motor, such as flux density, inductance, PM flux linkage and efficiency map. The demagnetization analysis of the ferrite magnet is also addressed to ensure the safety operation of the proposed motor. [http://dx.doi.org/10.1063/1.4974524]

I. INTRODUCTION

Due to the unique flux concentrating structure and no windings or magnets on the rotor, the flux switching permanent magnet machine (FSPMM) has the merits of high torque ability and good mechanical structure. Since the first flux switching alternators and the three phases FSPMM were proposed by S.E. Rauch in 1955 and E. Hoang in 1997, respectively, this kind of machine has under gone significant development in the past decades.[1] Various structures of FSPMMs have been investigated, including the E core, C core, multi-teeth, axial flux, transverse flux, axial laminated, outer rotor FSPMM using different electromagnetic analysis methods.[2–5] To enhance its ability for the high speed operation, the hybrid excitation method and mechanical flux regulated method were proposed as well.[6,7]

The soft magnetic composite (SMC) material is a relatively new soft magnetic material that can be used to design the electrical machines.[8,9] Compared with the traditional silicon steels, the SMC material has the benefits of low eddy current loss, low manufacturing cost, and 3D magnetic characteristic. As its merit of low manufacturing cost, it is possible to design a low cost electrical machine with SMC core. In terms of cost, among various kinds of permanent magnet (PM) materials, the ferrite magnet is very cheap but it has quite low magnetic energy product.[10,11]

Based on the good flux concentrating structure of FSPMM, this paper proposes a new 3D flux FSPMM (3DFFSPMM) with SMC cores and ferrite magnets. Compared with the traditional FSPMM,

[a]Chengcheng Liu, Email: chengchengliu1988@foxmail.com, and Youhua Wang, Email: wangyi@hebut.edu.cn

the new 3DFFSPMM can make utilizing of the 3D magnetic characteristic of SMC core to design the extended stator teeth and stator yoke to enhance the motor performance. Similar to the concept using of Halbach PM to enhance the main magnetic flux density of FSPMM that was proposed in ref. 12, this paper uses the radically magnetized PM and the outer stator back core to enhance the performance of the 3DFFSPMM. Moreover, the PM flux of the 3DFFSPMM can be regulated by rotating the outer PM in mechanical way, which will help the machine can be operated in the high speed region more efficiency.

II. TOPOLOGY OF 3DFFSPMM WITH SMC CORES AND FERRITE MAGNETS

Fig. 1(a) illustrates the topology of the 3DFFSPMM with SMC cores and ferrite magnets. Compared with the traditional FSPMM, the new 3DFFSPMM has extended stator teeth and yoke, outer PM and extended stator back core thus the machine can provide high flux density though the low cost ferrite magnets are adopted. Considering that the FSPMM with 6 stator cores and 7 rotor poles can provide the highest torque density when compared with FSPMMs of other configurations,[4] this paper chooses the same configuration. The flux switching operation principle of this machine is the same as that of the traditional ones. The added stator back core and the outer radial PM enable the 3DFFSPMM has higher flux density in the air gap than the traditional one, as shown in Fig. 1(b). Meanwhile, when the outer PM rotates with a determined shift angle, the PM flux generated by the PMs between the adjacent stator teeth will be reduced, and thus the effective PM flux linkage per winding will be lowered.

The main dimensions of the motor are tabulated in Table I. SOMALOY 500^{TM} is used to build the stator core and rotor core and the Y30BH ferrite is used for the magnets. The magnetic properties of SOMALOY 500^{TM} are obtained from our previous work.[9] The 3DFFSPMM is designed for low speed electric vehicle application. Its rated power is 3 kW and the maximum speed is 4200 rpm.

III. 3D FINITE ELEMENT ANALYSIS

To calculate the magnetic field and parameters of the 3DFFSPMM, the 3D FEM package MAXWELL is used.

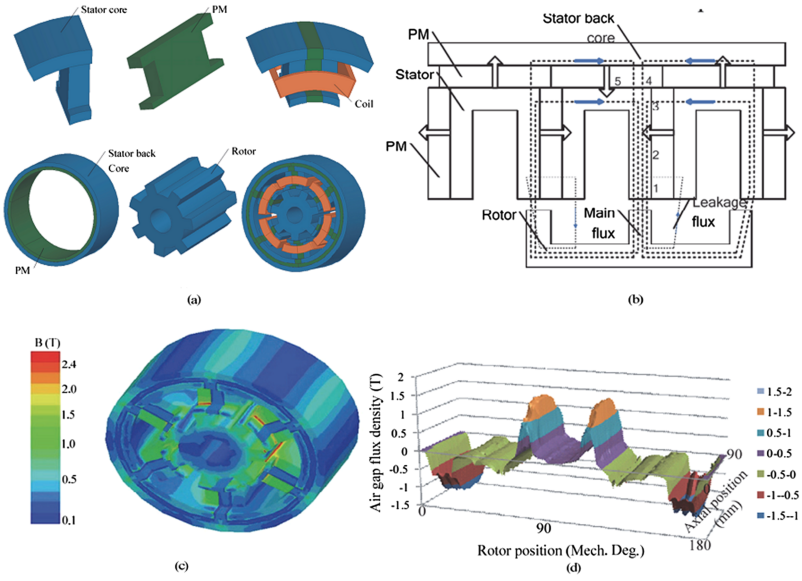

FIG. 1. (a) Topology of 3DFFSPM, (b) Main flux path, (c) No load flux density distribution, (d) Air gap flux density distribution.

TABLE I. Main Dimensions of the 3DFFSPMM.

Item	Value	Unit
Stator inner radius	46	mm
Inner stator outer radius	86	mm
Outer stator inner radius	92	mm
Outer stator outer radius	100	mm
Air gap length	0.5	mm
Shaft radius	15	mm
Inner PM width	12	mm
Axial length	90	mm
Axial length of stator assisted teeth	15	mm
Stator teeth width	12.8	mm
Rotor teeth width	14.3	mm
Rotor teeth height	12.3	mm

A. Magnetic field distribution

Fig. 1(c) shows the no load magnetic field distribution of the 3DFFSPMM. It can be found that the magnetic saturation occurs at the corner of the tips of stator tooth rotor tooth. Even though the low energy density ferrite magnet is used to produce the magnetic flux, the 3DFFSPMM can generate the maximum air gap flux of more than 1.4 T, as shown in Fig. 1(d). The air gap flux density under the extend teeth is around 0.8 T to 1 T.

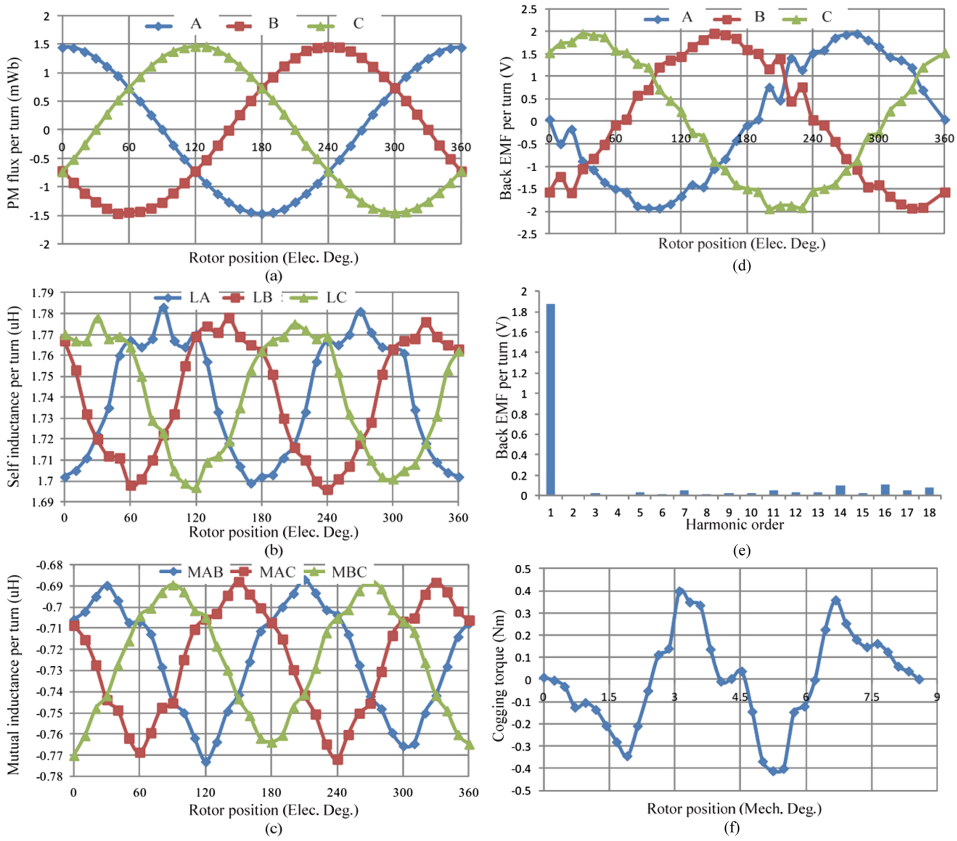

FIG. 2. (a) PM flux linkage per turn of 3DFFSPMM, (b) self inductance per turn, and (c) mutual inductance per turn of 3D FFSPMM, (d) waveforms of back EMF, (e) harmonics of back EMF, and (f) cogging torque waveform.

B. Flux, back EMF, inductance and cogging toque

The PM flux per turn and inductance per turn of the 3DFFSPMM are illustrated in Fig. 2 (a)–(c). It can be found that the PM flux per turn of 3DFFSPMM is around 1.5 mWb, and the average self-inductance per turn is around 1.74 μH. The number of coil turns is 12, and the rated phase current is 90A. The characteristic current can be calculated by

$$I_c = \psi_{pm} \Big/ L_d \tag{1}$$

where Ψ_{pm} is PM flux per windings and L_d the d-axis inductance per winding. In the 3DFFSPMM, the d-axis inductance is roughly 1.5 times as big as the self inductance. The calculated characteristic current is 48 A, which is much lower than the rated phase current of 90 A. Thus, this motor can operate to the infinite maximum speed theoretically. On the other hand, the power factor of this motor is quite low as the inductance is increased. Compared with the traditional FSPMM, the magnetic permanence of this motor is nearly doubled, thus the inductance is increased.

Fig. 2 (d)–(f) plots the back electromotive force (EMF) per turn at 1800 rpm and cogging torque of the 3DFFSPMM. For the 3DFSPMM is one kind of the FSPMM, its back EMF waveform is a basically sinusoidal waveform as shown in Fig. 2(d). However, it can find there are some fluctuates on the back EMF waveform that resulted by the nonlinear magnetic characteristic of the SMC material, it can be verified by the harmonic analysis result of the back EMF as shown in Fig. 2(e). The magnitude values of the fundamental component of the back EMF is 1.83 V. Since the designed maximum speed of the motor is 4200 rpm, which corresponds to the maximum frequency of 490 Hz, the skin effect depth of the coil is 2.9 mm. Therefore, it is necessary to use the multi-strand winding to reduce the AC resistance. The calculated copper resistance is 0.0029 ohm, and the slot fill factor is 0.62.

IV. PERFORMANCE ANALYSIS

A. Operation characteristic

To judge the performance of a machine, the efficiency map is a useful tool, as it can show all the operation information, as shown in Fig. 3(a). To plot this map, the efficiency with the different output torque and rotor speed should be calculated. In this paper, the control strategy that d-axis current equals zero is used, though the designed 3D-flux FSPMM with the flux weakening control can achieve the infinite maximum speed theoretically. It should be noted that the efficiency map can be different with the different control strategies. In Fig. 3(a), the speed below 2400 rpm shows the constant torque operation region of the 3DFSPMM, the speed between 2400 rpm and 4200 rpm shows the reduced power operation region, and the contour lines show the operation efficiency of this motor under the different speed and torque.

The output torque and efficiency can be expressed as,

$$T_{out} = (P_{em} - P_{Core} - P_{pm} - P_{mech})/\omega_r \tag{2}$$

$$\eta = P_{out}/(P_{em} + P_{cu}) \tag{3}$$

where P_{em} is the electromagnetic power, P_{Core} the core loss, P_{pm} the PM loss, P_{mech} the mechanical loss, ω_r the rotor speed, and P_{out} the output power. The electromagnetic power can be calculated based on the 3D magnetic field FEM and $T_{em} * \omega_r/9.55$. The permanent magnet loss can be estimated as zero since the resistivity of ferrite magnet is very high. The mechanical loss is estimated as the 1.5% of the output power. For the calculation of core loss, the multi frequency core loss properties of SMC material are used. The copper loss of the machine can be calculated by $3I^2R$.

B. Mechanical flux regulation ability

Besides the PM flux contributed by the outer PM can enhance the torque ability of the 3DFFSPMM, the outer PM can also be used to reduce the PM flux by shifting it with a determined angle from its original position. The PM flux per turn of the 3DFFSPMM with different shift angle is shown in the Fig. 3(b). As shown, the PM flux can be decreased when the shift angle increases;

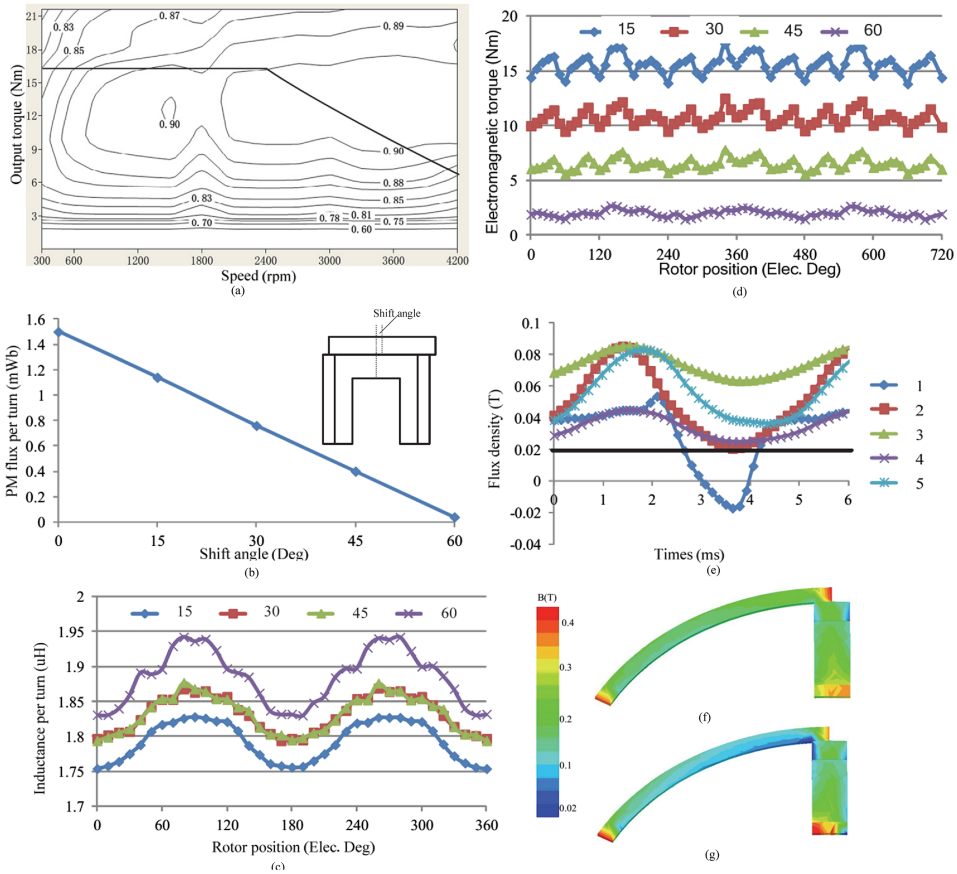

FIG. 3. (a) Efficiency map of the 3DFFSPMM, (b) PM flux per turn with the shift angles increases, (c) Inductance per turn with the shift angles increases, (d) Electromagnetic torque with the shift angles increases, (e) Demagnetization analysis of the machine at the peak load and temperature of 24 °C, (f) and (g) Demagnetization analysis of the machine at two typical times under the temperature of 24 °C: (f) at the times of 1.5 ms, and (g) at the times of 3.8 ms.

it approaches to 0 when the shift angle equals 60 degs. The definition of the shift angle is shown in Fig. 3(b).

Fig. 3(c) shows the inductance per turn of the 3DFFSPMM with different shift angles. The overlapping of the inductances with shift angle of 30 and 45 degs is resulted by the nonlinear permeability of the SMC material since the inductance is highly depend on the magnetic flux density distribution of the motor. The general trend of the inductance can be concluded as it will increase with the shift angle increases, however it may be kept unchanged when the shift angle has a slight increase when the shift angle is between 30 and 45 degs. As shown in Fig. 1(b), all the PM flux from both PM and outer PM will be utilized to produce torque when the shift angle equals zero, while the PM and outer PM can form a closed flux path when the shift angle equals 60 degs and the main flux will be wasted to produce the torque. Fig. 3(d) shows the electromagnetic torque of the 3DFFSPMM in terms of shift angle, which is resulted by the relationship between the PM flux per turn and shift angle. It can be seen that the average of the torque will be decreased as well with the increasing of the shift angle.

C. Demagnetization checking

Since the ferrite magnet is more susceptible than the NdFeB PM, the demagnetization characteristic of the 3DFFSPMM is checked for the room temperature of 24 °C. According to the demagnetization curve of the Y30H, 0.02 T is the reference knee point flux density at 24 °C. Five typical points the PM are chosen for the demagnetization analysis when the peak load is applied, as shown in Fig. 1(b). As shown in Fig. 3(e), the partially demagnetization of the PM is occurred at the point of 1 when

the time is between 2.5 ms and 4 ms. Fig. 3(f) and (g) illustrate the magnetic field distribution along the magnetization direction on the ferrite magnets at two typical times (1.5 ms and 3.8 ms) under the room temperature of 24 °C.

V. CONCLUSION

In this paper, a new 3DFFSPMM with SMC cores and ferrite magnets is proposed and analyzed. By taking the advantage of high freedom design of the SMC material, the end region, outer PM and outer stator back of the machine can be both utilized to enhance the performance. In addition, the outer PM in the 3DFFSPMM can be used to regulate the PM flux in mechanical way. The optimal control of the 3DFSPMM is very complex which will be continued in our future work, however, the mechanical flux weakening control can improve the operational efficiency and the maximum operational speed of the 3DFSPMM. This 3DFFSPMM is designed for the low speed micro electric vehicle application. It can be argued that both the material cost and manufacturing cost of the designed 3D flux FSPMM is quite low. By using the 3D FEM package MAXWELL, its main magnetic parameters and machine performance have been predicted under both the normal and flux weakening operation state. The demagnetization analysis is completed to check the machine design and it is found that the 3DFFSPMM can operate safely though some areas can be partially demagnetized.

[1] M. Cheng, W. Hua, J. Zhang, and W. Zhao, IEEE Trans. Ind. Electron. **58**, 5087 (2011).
[2] J. H. Yan, H. Lin, Z. Q. Zhu, P. Jin, and Y. Guo, IEEE Trans. Magn. **49**, 2169 (2013).
[3] M. Lin, L. Hao, X. Li, X. Zhao, and Z. Q. Zhu, IEEE Trans. Magn. **47**, 4457 (2011).
[4] W. Xu, G. Lei, T. Wang, X. Yu, J. Zhu, and Y. Guo, IEEE Trans. Magn. **48**, 4050 (2012).
[5] J. T. Chen, Z. Q. Zhu, and D. Howe, IEEE Trans. Magn. **44**, 4659 (2008).
[6] W. Hua, G. Zhang, and M. Cheng, IEEE Trans. Magn. **50**(11) (2014).
[7] Z. Q. Zhu and J. T. Chen, IEEE Trans. Magn. **46**, 1447 (2010).
[8] J. G. Zhu, Y. G. Guo, Z. W. Lin *et al.*, IEEE Trans. Magn. **47**, 4376 (2011).
[9] C. C. Liu, J. G. Zhu, Y. H. Wang *et al.* **117**, 17B507 (2015).
[10] Y. Guo, J. Zhu, and D. G. Dorrell, IEEE Trans. Magn. **45**, 4582 (2009).
[11] G. Lei, Y. G. Guo, J. G. Zhu, T. S. Wang, X. M. Chen, and K. R. Shao, IEEE Trans. Magn. **48**, 923 (2012).
[12] C. Walter, H. Polinder, and J. Ferreira, IEEE Trans. JESTPPE. **1**, 327 (2013).